JOURNAL OF MATERIALS SCIENCE 17 (1982) 1156–1166

Solid-state polymerization of tricosa-10,12-diynoic acid

B. TIEKE*†, D. BLOOR*, R. J. YOUNG‡
Department of Physics and Department of Materials‡, Queen Mary College, Mile End Road, London E1 4NS, UK*

The γ-ray polymerization of tricosa-10,12-diynoic acid ($CH_3-(CH_2)_9-C\equiv C-C\equiv C-(CH_2)_8-COOH$) crystals has been studied by X-ray diffraction, optical- and scanning electron-microscopy and Raman- and optical-spectroscopy. Up to a conversion of about 60%, the bulk of the polymerization proceeds in a homogeneous single phase. Above about 50% conversion a phase transition, nucleating at crystal defects, occurs. Defect free crystals, which remain in the initial phase above 60% conversion, can be transformed by mechanical deformation. The transformation to the new phase destroys the macroscopic crystalline order but allows further polymerization at a reduced rate.

1. Introduction

It has been known for a number of years that the solid-state polymerization of single crystals of disubstituted diacetylenes initiated by heat, ultraviolet (u.v.) irradiation or ionizing radiation can lead to the formation of macroscopic polymer single crystals [1–3]. The physical properties of these materials have attracted considerable attention as the fundamental properties of the extended, conjugated polymer chains can be studied free from the high defect densities present in amorphous and partially crystalline materials [4–6].

The packing of monomer molecules into ordered arrays suitable for solid-state polymerization can be achieved in single crystals, inclusion compounds, layer perovskites, monomolecular layers and Langmuir–Blodgett (L–B) multilayers [7–10]. Although there have not yet been any major studies of the polymerization of intercallated diacetylenes, there have been numerous reports of the polymerization of mono- and multilayers of amphiphilic diacetylene monocarbonic acids [11–27].

Despite this activity and studies of the complexes formed between phenazine and 2, 4-diynoic acids [28–30], only brief reports have appeared of the polymerization of the pure acids [12, 31]. One of the first papers was published in 1940 and deals with the isolation of the naturally occurring erythrogenic acid which is described as forming a blue and finally red, insoluble product, dependent on the u.v. irradiation dose [32].

We report here an extensive investigation of the solid-state polymerization of single crystals of tricosa-10,12-diynoic acid (TCDA: $CH_3-(CH_2)_9-C\equiv C-C\equiv C(CH_2)_8-COOH$). This monomer is a typical example for the amphiphilic diacetylene fatty acids, with long paraffinic sequences on either side of the diacetylene moiety, which have been used in the formation of polymerizable monolayers and L–B-multilayers [15].

2. Experimental procedure

TCDA monomer was synthesized by a Cadiot–Chodkievicz coupling of the 1-iodo-1-alkyne and the 10-undecynoic acid as described in detail elsewhere [15]. This method gave yields of 55 to 60 %. Single crystals in the form of thin rectangular platelets with dimensions up to 5 mm × 3mm × 0.1 mm were grown by slow evaporation from petroleum ether (boiling point 60 to 80° C). The crystal melting point was 57° C and the chemical composition was as expected for

---

†Present address: Institut für Makromolekulare Chemie, Stefan Meier Straße 31, D-78 Freiburg, West Germany.

0022–2461/82/041156–11$03.82/0

TABLE I Unit cell dimensions of diynoic acids and phenazine–diynoic acid complex monomers.

Material	a^* (nm)	b (nm)	c (nm)	α(°)	β(°)	γ(°)
TCDA	0.476(4)	0.542(4)	4.23(8)	90 ± 1	90 ± 1	95.2 ± 0.2
HDDA	0.491(4)	0.536(5)	3.27(1)	90.5 ± 0.2	91.6 ± 1	106.7 ± 1
HDDA–Ph	0.477(4)	0.709(5)	3.32(1)	91.5 ± 0.2	91.6 ± 1	104.5 ± 1
NDDA–Ph	0.474(4)	0.715(5)	3.64(1)	84.1 ± 0.2	92.1 ± 1	106.1 ± 1

* The standard deviations of the value of the least significant digit of the lattice dimensions are shown in brackets.

$C_{33}H_{38}O_2$ (calculated: C = 79.77 wt %, H = 10.98 wt %; found: C = 79.82 wt %, H = 11.00 wt %).

The monomer crystals were polymerized by irradiation with ^{60}Co-γ-rays using doses up to 120 Mrad. The degree of conversion to polymer was determined gravimetrically by dissolving the residual monomer in $CHCl_3$, with vigorous stirring to ensure complete dissolution of the monomer at the higher levels of conversion. The polymer was filtered with pre-weighed glass frits and was dried to constant weight, a technique which has given accurate results with other diacetylene crystals [33, 34].

X-ray diffraction determination of the monomer unit cell dimensions was executed using photographic methods. Oscillation, zero- and first-layer Weissenberg photographs were taken using Ni-filtered CuKα radiation. Despite the fact that the exposures were kept as short as possible, deterioration of the crystals after a few hours X-ray exposure indicated that some polymerization had occured.

Raman spectra were recorded at 300 K using excitation radiation from a Coherent Radiation dye laser operated with Rhodamine 6G dye. The scattered light was analysed with a Spex double monochromator fitted with an RCA 3300 photomultiplier. The photomultiplier was cooled to reduce the background count level. The output was fed to a Brookdeal–Ortec photo-counting system and analogue recorder. Laser power levels were kept below 10 mW to prevent degradation of the samples. At this power level the resolution was typically 4 cm^{-1}.

Optical spectra were recorded using a Pye Unicam SP 1800 u.v. visible spectrophotometer with a spectral bandwidth of 1 nm. Low temperature spectra of a partly polymerized crystal were obtained by mounting the sample in an Oxford Instruments continuous flow cryostat which could be controlled at any temperature between 10 and 300 K.

Optical micrographs were taken on a Zeiss Universal Research microscope. Scanning electron micrographs (SEMs) were recorded with a JEOL ISM 50A scanning electron microscope. Samples were selected by optical microscopy, mounted on aluminium stubs and gold coated prior to SEM observations.

3. Results and discussion

3.1. X-ray diffraction

TCDA crystals are monoclinic with the unit cell parameters listed in Table I. Better values could not be obtained since the best crystals of a size suitable for X-ray diffraction studies were so thin that they easily deformed, producing streaks in the Weissenberg diagram, as shown in Fig. 1. Exposure to X-rays produced further deterioration of these patterns and it was not possible to obtain useful photographs of crystals with a large polymer content.

The lattice cell dimensions of TCDA are comparable with those of the heptadeca-2, 4-diynoic acid (HDDA) and the phenazine complexes formed from HDDA and nonadeca-2, 4-diynoic acid (NDDA) [30], see Table I. The values of a for all these materials are similar, as are the b-values for the pure acids. The larger value of b for the phenazine complexes is due to the larger tilt angle of the long acid molecules necessary to accomodate them plus the phenazine molecule within a constant layer (c-axis) spacing. The c-axis dimensions reflect the differences in length of the acid molecules. However, TCDA is monoclinic in comparison with the triclinic structures of HDDA and the phenazine complexes.

These facts reflect the way in which the crystal structure is primarily determined by the packing of the long-chain paraffinic sequences of the diacetylene substituent groups. Their effect is greatest in TCDA, which, of the compounds listed in Table I, has the longest paraffin chains giving a more symmetric packing closer to the orthorhombic structure found in paraffin molecules containing an odd number of carbon atoms.

From the lattice cell parameters we can conclude that the TCDA molecules pack in a head-

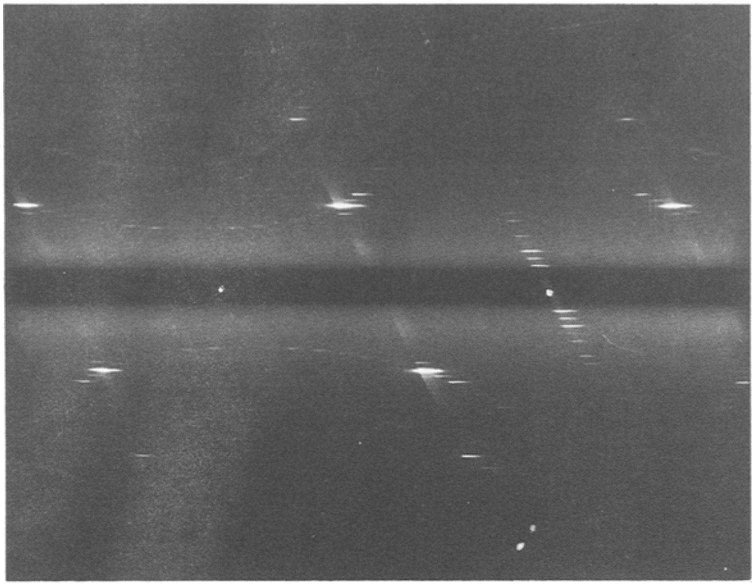

Figure 1 Zero-layer Weissenberg photograph of a TCDA-monomer single crystal recorded at 300 K with Ni-filtered CuKα radiation.

head-tail-tail layer arrangement as found for HDDA, NDDA [30] and L–B-multilayers [12]. Since the molecular length of TCDA, calculated using established bond lengths [35], is about 3.06 nm, the molecules must lie at an angle of about 45° to the layer plane.

3.2. Polymerization

Despite the fact the a monomer separation of 0.476 nm and a tilt angle of 45°, with respect to the stack of monomers, is close to the limit set by the van der Waals atomic radii and well within the limits for solid-state reactivity [3, 36, 37], TCDA crystals do not polymerize thermally, Since the penetration depth of u.v.-radiation active in photopolymerization is very small, it is necessary to use penetrating ionizing radiation to obtain quantitative conversion data. The results obtained for the ^{60}Co-γ-ray polymerization of TCDA crystals at room temperature are shown in Fig. 2.

The polymerization curve for TCDA is similar to that reported for NDDA and the NDDA–phenazine complex [30] with an initial rapid increase in polymer content. However, the rate of polymerization decreases at higher doses and

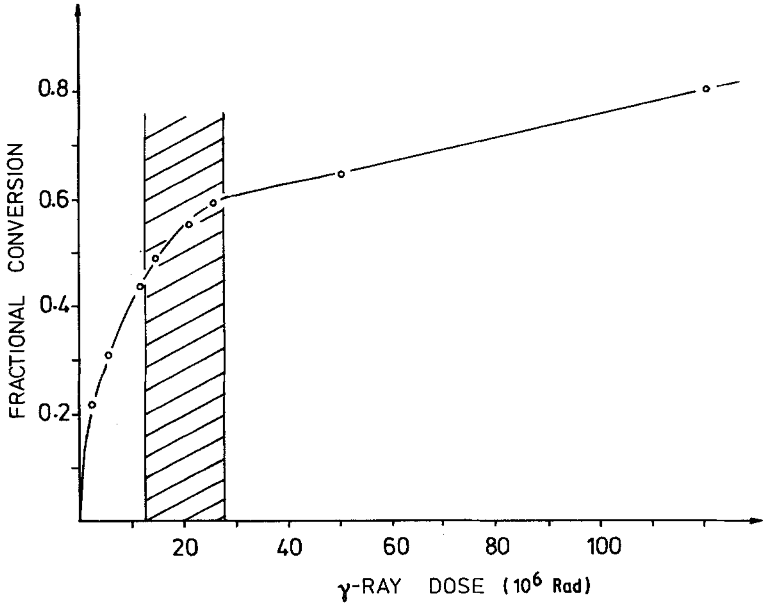

Figure 2 Conversion against dose curve for TCDA-crystals polymerized at 300 K with ^{60}Co-γ-ray radiation. The region in which a disruptive phase transition occurs is shown by the vertical shaded area.

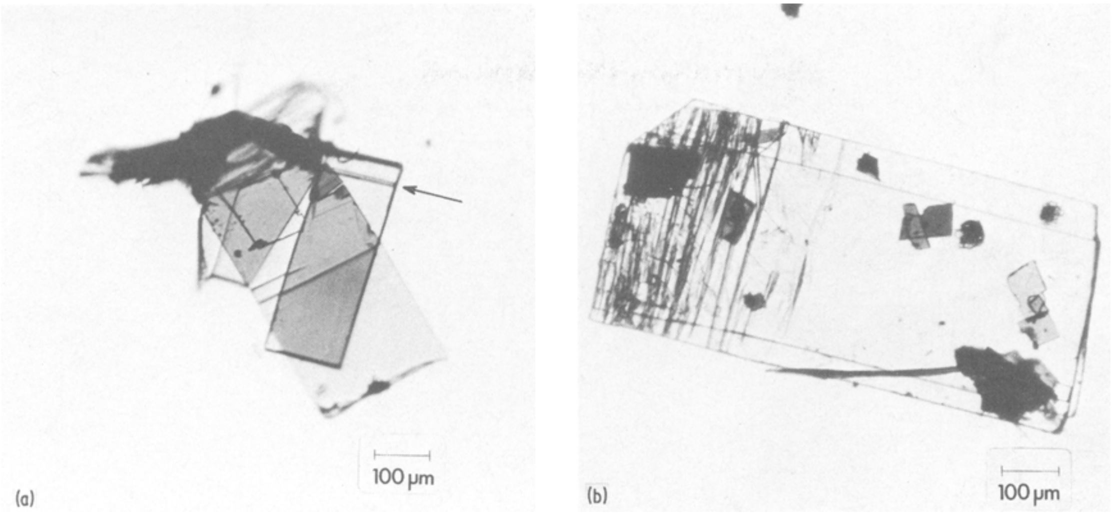

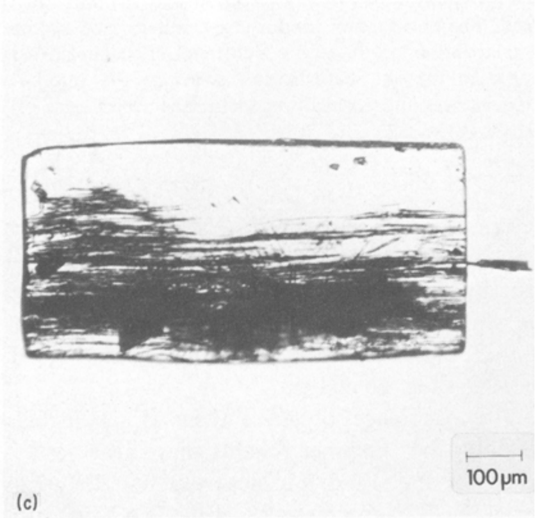

Figure 3 Optical micrographs of TCDA-crystals subjected to a ^{60}Co-γ-ray dose of 20 Mrad showing (a) low, (b) moderate and (c) high levels of deformation due to the disruptive phase transition. The arrow in (a) points to a deformation twin introduced by external stress.

becomes small, and approximately constant, for doses in excess of 20 Mrad, i.e. above 60 % conversion to polymer. The rate of polymerization of TCDA above 60 % conversion is much larger than that observed for either NDDA or the NDDA–phenazine complex. This continuing polymerization is accompanied by disruption of the TCDA crystals; in contrast the NDDA–phenazine complex retains its single-crystal form, but polymerization beyond 65% conversion is negligible.

We believe that these facts indicate a gradually increasing strain in the pure acid crystals during polymerization due to the presence of hydrogen bonding between the acid groups opposing the dimensional changes resulting from polymerization. Finally, this strain is relieved by disruption of the crystals, probably due to the formation of a new phase, and polymerization can continue though at a much reduced rate.

In contrast in the NDDA–phenazine crystals hydrogen bonds between the acid molecules and the phenazine are likely. These hydrogen bonds are also much closer to the reacting diacetylene units than in TCDA. These differences lead to a stable state for the NDDA–phenazine complex crystals at 65 % conversion when the strain energy is insufficient to drive a transition to a more reactive modification and further polymerization leads to an overall increase in free energy of the crystal. The lower strain energy may result from a more facile movement of the carboxylic groups than in TCDA crystals because of the interposition of the phenazine molecules between the acid molecules.

3.3. Microscopy

Optical and SEM observation of TCDA crystals after 8, 20, 26, 34 and 50 Mrad radiation doses confirmed that they are disrupted at high levels of conversion to polymer. However, it was found that this was dependent on the defects and strain in the monomer crystals since at all levels of irradiation small crystals could be found free from the cleavage and deformation present in large crystals. Typical optical and scanning electron micrographs are shown in Figs 3 to 6.

All the crystals studied after a dose of 8 Mrad

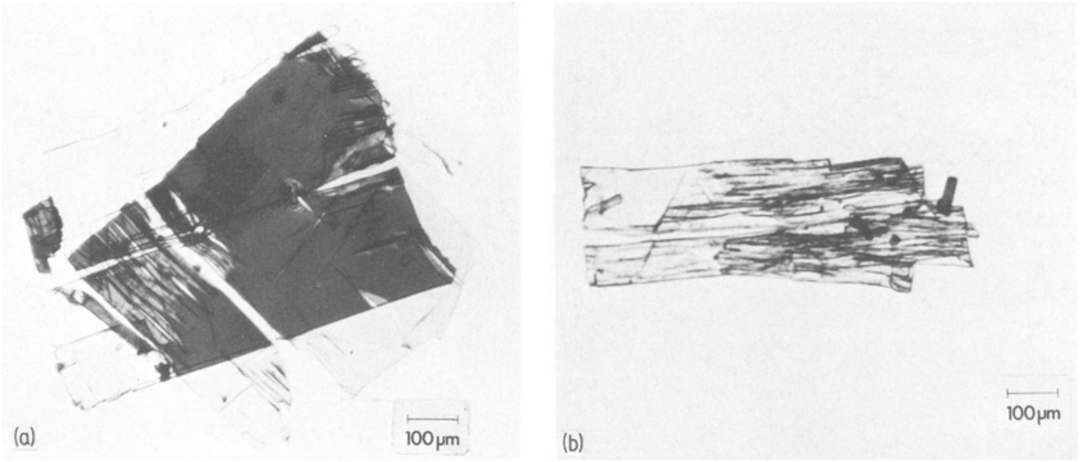

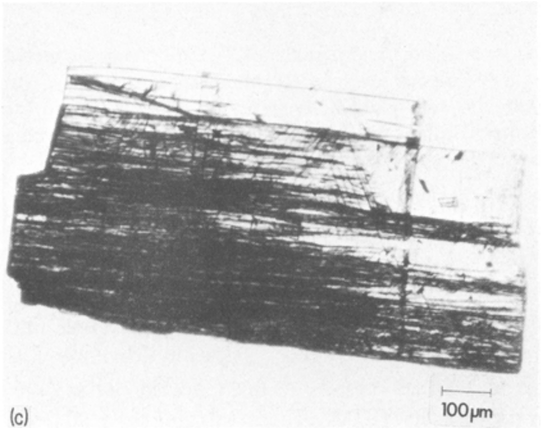

Figure 4 Optical micrographs of TCDA-crystals subjected to ^{60}Co-γ-ray doses of (a) 26 Mrad and (b) and (c) 34 Mrad. The polarization produced by undeformed and the depolarization produced by deformed crystal regions is visible in (a) and deformation twins at the interface between the undeformed and deformed regions are evident in (b) and (c).

were highly perfect platelets; in only one case was a small cleavage crack found, see Fig. 5a. After 20 Mrad dose the degree of disruption of the crystals varied considerably, typical optical micrographs of crystals with little, moderate and considerable deformation are shown in Fig. 3a, b and c, respectively. As the dose was increased, the number of crystals with moderate to heavy damage increased, crystals observed after doses of 26 and 34 Mrad are shown in Fig. 4. The sample subjected to 50 Mrad of γ-irradiation had a much smaller average crystallite size than those given lower doses. Under the optical microscope this sample was seen to consist of agregates of deformed crystals and very small undeformed crystals. Such undeformed crystals as observed in the SEM are shown in Fig. 5c.

Two modes of deformation are observed, in which cracks propagating along the polymerization direction (a-axis) either simply result in deformation of the crystal in a gradual way or are associated with stress twins at the interface between deformed and undeformed crystal. The former mode results in a depolarization of transmitted light by the disordered polymer, as shown in Fig. 4a while the latter results in series of structures at the boundary of the deformed region, Fig. 3b and c and Fig. 4b and c.

The occurence of stress twins which involve bending the polymer chains has been established in the 1,6-di-p-toluenesulphonoyloxy-2,4-hexadiyne(TS)-polymer [38–40]. The twins produced by the deformation in TCDA make an angle of about 60° to the a-axis which requires twins with traces of $(2\,1\,0)$ and $(\bar{2}\,1\,0)$ planes on the crystal a–c-face. However, though the twins in TS produce distinct steps on the crystal facets, those observed in TCDA produce only narrow features on the a–c-face, see Fig. 6b, c and d. Occasionally cracking occurs along the twin plane, see Fig. 6d, this presumably occurs either at a relatively low conversion or in a region of high residual monomer content, in either case insufficient polymer chains exist in the region of the crack to prevent failure of the crystal. One crystal subjected to 20 Mrad irradiation was observed to deform under external stress to produce a twin with a well defined width and a trace along the $(0\,1\,0)$ plane; this is indicated by the arrow in Fig. 3a.

Other features occur on the crystal surfaces,

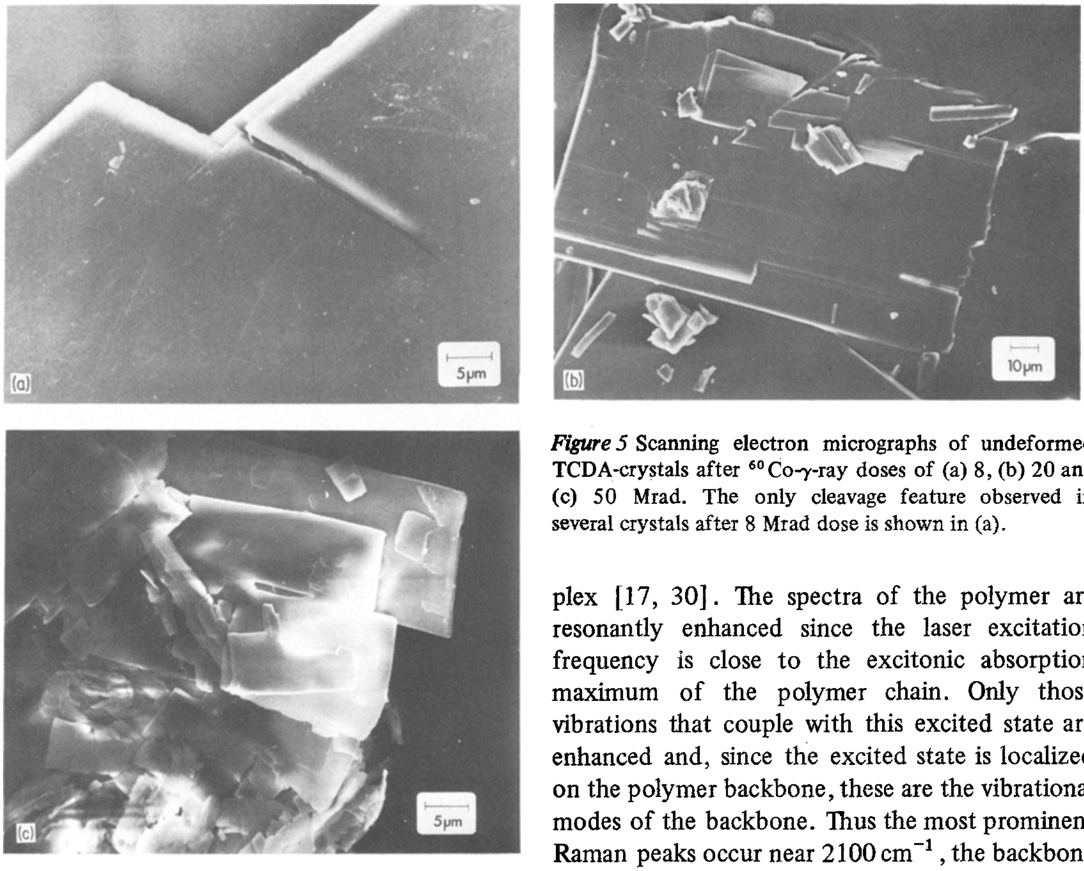

Figure 5 Scanning electron micrographs of undeformed TCDA-crystals after ^{60}Co-γ-ray doses of (a) 8, (b) 20 and (c) 50 Mrad. The only cleavage feature observed in several crystals after 8 Mrad dose is shown in (a).

e.g. Fig. 5b, but these have a different orientation, corresponding to (110) planes; since they are observed for low γ-ray dose, these are presumably crystal growth features.

Clearly the occurence of deformation is sensitive to the perfection of the TCDA crystals. This is not unexpected since nucleation of a new crystal phase is likely to occur either at crystal defects or in highly strained regions of the crystal. However, it is not possible to determine the exact mechanism from the microscope data. Detailed analysis of the twinning is not possible due to the absence of information concerning the crystal structure of TCDA and the deformation of the polymer chains in the twinned regions.

3.4. Raman spectroscopy

Raman spectra recorded with a laser excitation frequency of 16 103 cm^{-1} for samples with less than 0.1, 12 and 20 Mrad doses of ^{60}Co-γ-rays are shown in Fig. 7. The spectra are similar to those previously reported by us for TCDA–Cd-salt L–B-multilayers, HDDA and HDDA–Ph complex [17, 30]. The spectra of the polymer are resonantly enhanced since the laser excitation frequency is close to the excitonic absorption maximum of the polymer chain. Only those vibrations that couple with this excited state are enhanced and, since the excited state is localized on the polymer backbone, these are the vibrational modes of the backbone. Thus the most prominent Raman peaks occur near 2100 cm^{-1}, the backbone C≡C-stretching mode [41, 42]. The backbone modes at lower frequencies display Fermi resonances with a number of vibrations of the paraffinic side-groups leading to a complex structure, which is dependent on the lengths of the paraffinic side chains attached to the polymer, between 1400 and 700 cm^{-1}. At the lowest conversions a weak peak can be observed at 2143 cm^{-1} due to the C≡C-stretching mode of the monomer, its lower strength reflects the fact that it is not resonantly enhanced.

The C≡C-stretching frequency of the initially formed TCDA polymer is 2100 cm^{-1}, and this falls with increasing conversion to 2078 cm^{-1}, after 20 Mrad dose. The C=C-frequency changes only slightly from 1452 cm^{-1} at 0.1 Mrad to 1455 cm^{-1} at 20 Mrad. These changes are comparable with those observed for the HDDA–Ph complex and the TCDA–Cd–salt multilayers [31]. This indicates that all these systems undergo a homogeneous polymerization in the initial phase of polymerization. At 12 Mrad dose a new set of Raman peaks appears at 2120 and 1510 cm^{-1}. At a dose of 20 Mrad these have increased in intensity and shifted to 2123 and 1515 cm^{-1},

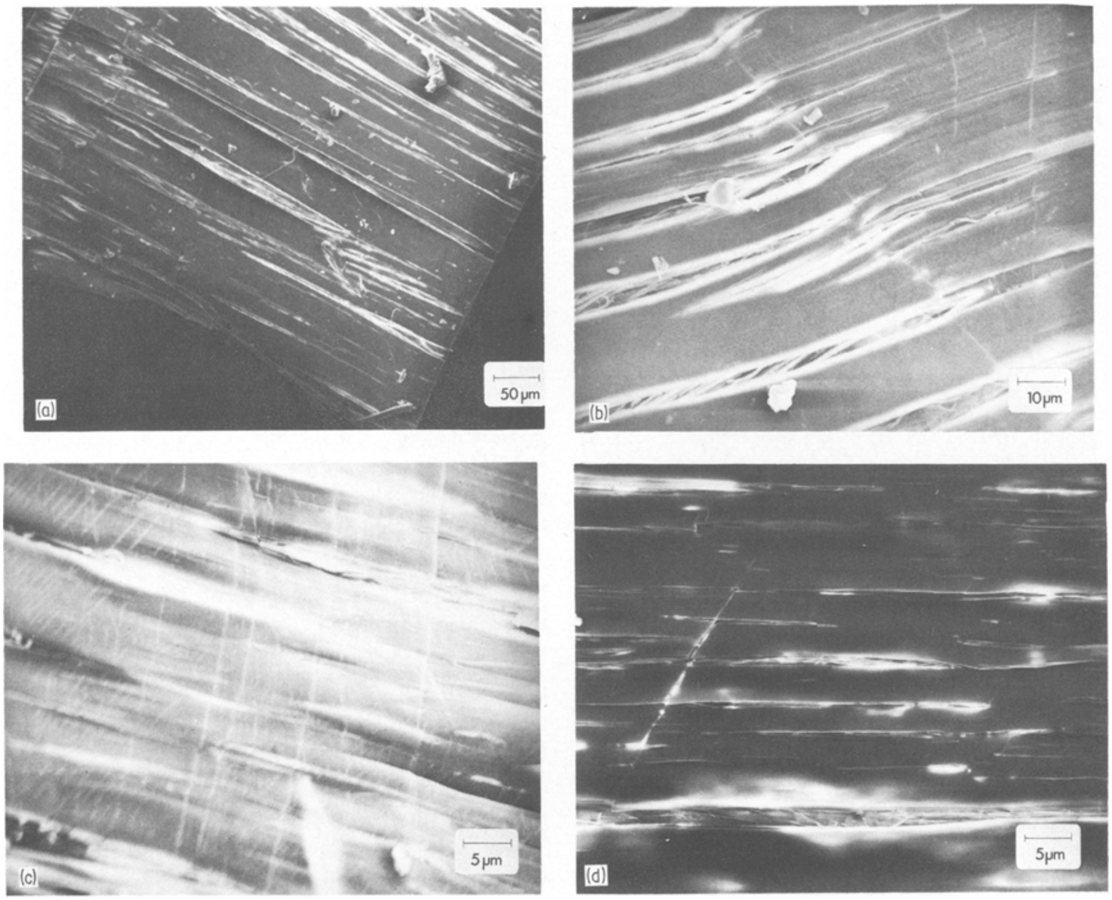

Figure 6 Scanning electron micrographs of deformed TCDA crystals after ^{60}Co-γ-ray doses of (a), (b) 20, (c) 26 and (d) 34 Mrad. Deformation twins appear as the narrow features in (b), (c) and (d). A crack along such a twin is visible in (d). The major cleavage is along the a-direction; polymer fibrils occur within these cleavage cells.

while the initial peaks have almost disappeared. The new peaks reveal the presence of a heterogeneously nucleating phase which is subjected to strain by the as yet undeformed initial phase, this strain being reduced when the bulk of the sample has converted to the new phase.

The Raman spectra show clear evidence for the initial homogeneous polymerization in the monomer crystal lattice. The growth of new Raman bands with a discontinuous shift from those of the initially formed polymer show that a transformation of the lattice to form a new crystal phase occurs. Though visual and optical microscope observations indicate a highly deformed morphology due to the disruption of the crystal structure by the formation of the new phase, the detail observable in the Raman spectrum, see Fig. 7, shows that considerable local order remains. This accords with the SEM observation of small well-ordered crystal regions separated by cleavage cracks bridged by a small number of polymer fibres (see Fig. 6).

3.5. Optical spectroscopy

The intense colouration of reactive di-substituted diacetylene crystals is due to the occurence of an excited excitonic state of the polymer backbone in the visible spectral region. The energy of the exciton is sensitive to the length of the polymer chain [43] and its conformation, which is largely determined by its environment in the crystal lattice [44]. In general, in both thermally and radiation polymerized samples the polymer chains are so long that the effect of the chain length on the absorption energy is negligible and the exciton absorption has a well defined structure with a line width which becomes much smaller at low temperatures.

As can be seen in Figs 8 and 9 the spectra of both macroscopic and microscopic TCDA

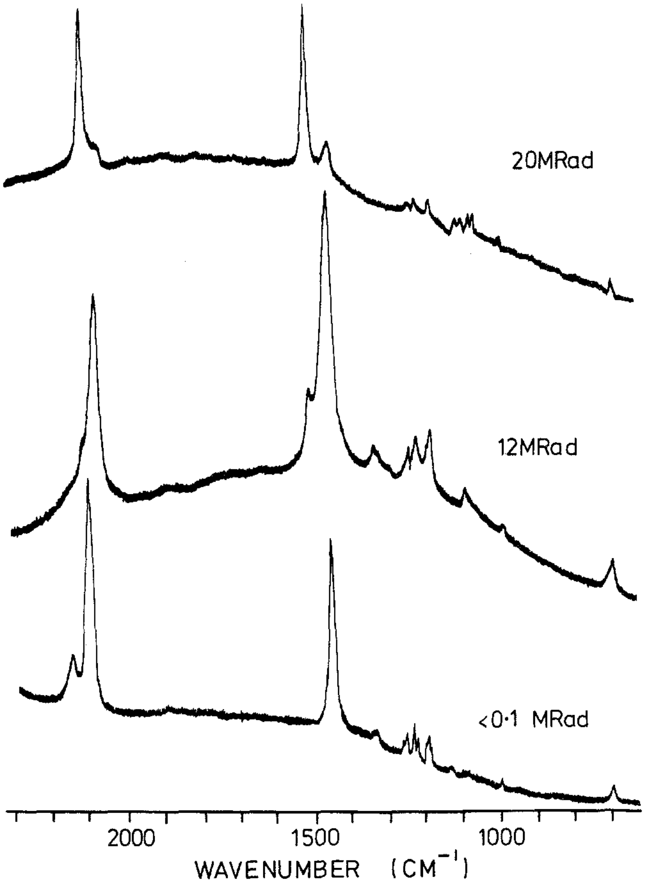

Figure 7 Raman spectra of TCDA-crystals as a function of ^{60}Co-γ-ray dose. The spectra were recorded at 300 K under the conditions described in the text.

crystals containing small quantities of polymer have well defined excitonic absorption bands. As the temperature of the single-crystal sample is decreased, the absorption lines sharpen and move to lower energies, see Figs 8 and 10. The large temperature dependence of the absorption has been reported for other diynoic acids containing small amount of polymer [30, 44]. This is due to the large thermal expansion coefficients of the monomer crystals, which are a consequence of large-amplitude thermal motion of the paraffinic chain at and above room temperature. In pure paraffins and polyethylene large anisotropic expansion coefficients are observed, that along the *a*-axis of the orthorhombic cell being ten times that along the *b*-axis [45]. Measurements of the unit cell parameters of the NDDA–Ph complex show a large contraction along the *a*-axis at low temperatures and comparable shifts in the optical absorption energy with those of TCDA shown in Fig. 10 [30]. Since the room-temperature values for the *a*-axis lattice parameter are similar for TCDA and the NDDA–Ph complex we conclude that the similarities in the optical spectra result from a similar compression of the initially formed polymer chains by the contraction of the monomer lattices in both cases. This conclusion is consistent with the increase in exciton energy observed for TS polymer fibres in extension [46].

Diffuse reflection spectra of samples subjected to a variety of treatments are shown in Fig. 9. At low conversion the diffuse reflection spectrum of microcrystalline material is essentially identical to the absorption spectrum of single crystals (cf. Fig. 8). The spectrum of a microcrystalline sample subjected to a 26 Mrad dose of ^{60}Co γ-rays retains a feature at long wavelengths but has a new reflection peak at 580 nm. This is in accord with the Raman spectra of Fig. 7, and the micrographs of Section 3.3, which show only residual traces of the initial phase at doses in excess of 20 Mrad. However, since the polymer content of the sample at a dose of 26 Mrad is high, i.e. ~60%, the simple Kubelka–Munk relation between diffuse reflectivity and absorption coefficient breaks down due to contributions to the scattering from the specular reflection of the sample. Thus, though the structure below 580 nm is suggestive

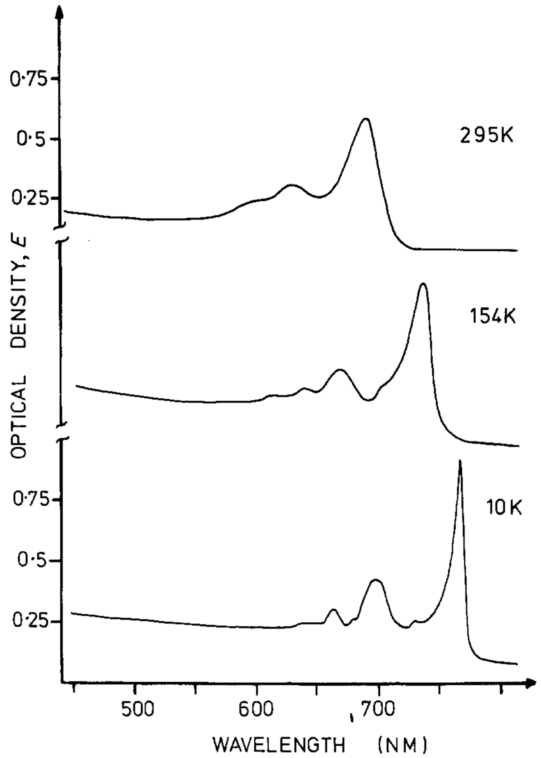

Figure 8 Transmission spectra of a TCDA single crystal containing less than 1 % polymer as a function of temperature.

of an exciton absorption and associated vibronics the energy assigned to the exciton absorption must be regarded as an approximate value.

When the irradiated sample is subjected to mechanical deformation there is a large increase in the shorter wavelength reflection peak, see Fig. 9. We conclude, therefore, that initially the sample contained a number of small, perfect crystallites that had remained in the initial phase and that the mechanical deformation resulted in the transformation of most of these crystals. The features below 580 nm remain after this treatment, confirming their assignment to the exciton and its vibronics of the new phase appearing above 60 % polymer content. The appearance of structure here and in the Raman spectra indicates that the bulk of the sample remains in an ordered state in the new phase despite the loss of macroscopic order.

This conclusion is further supported by the rather different spectrum observed for polymer samples obtained either by separating the polymer from the monomer at low levels of conversion, see Fig. 9, or by precipitation from a solution of TCDA-polymer in cyclohexanone [47]. The polymer in such samples is highly disordered and can adopt a conformation determined by interaction within and between isolated polymer chains. Such structures will clearly differ from those which have been either determined or influenced by the monomer crystal structure, as shown recently in the case of TS polymer [48].

4. Conclusions

Using a variety of experimental techniques, it has been shown that the γ-ray polymerization of

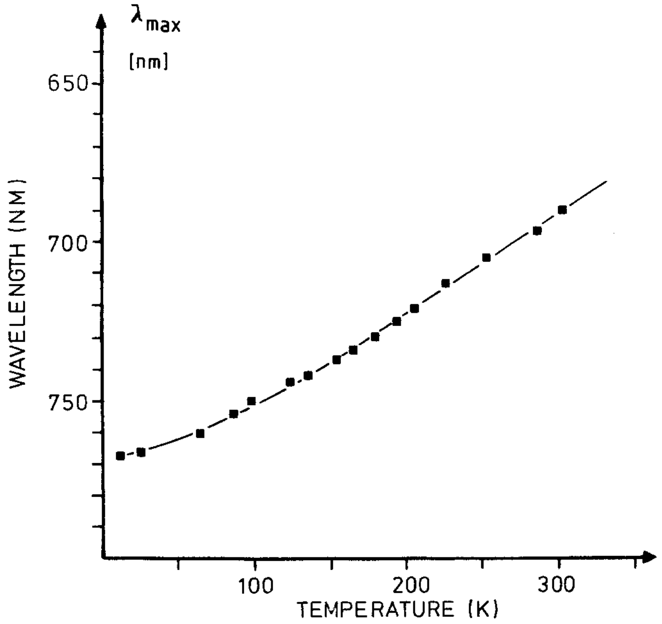

Figure 9 Diffuse reflection spectra for TCDA samples: I, microcrystals after less than 0.1 Mrad ^{60}Co-γ-ray dose, II microcrystals after 26 Mrad dose, III Sample II after mechanical deformation, and IV polymer extracted from Sample I.

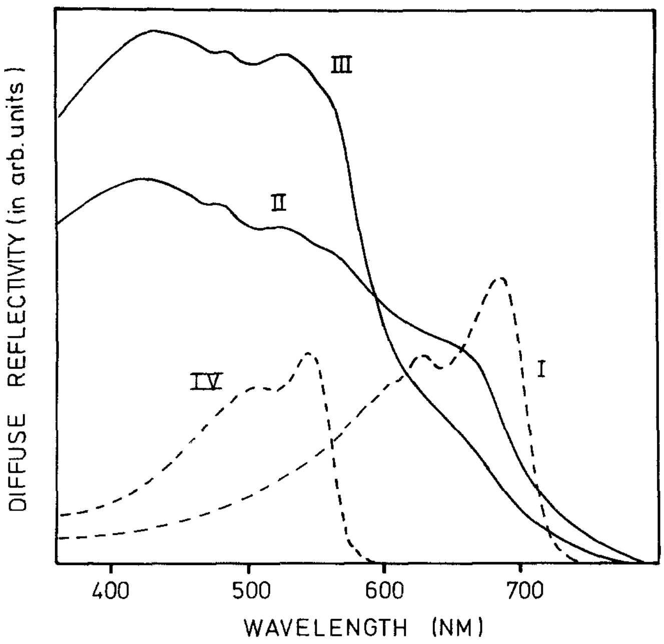

Figure 10 Temperature dependence of the excitonic absorption of TCDA-polymer in TCDA-monomer crystal matrix (polymer content less than 1 %).

TCDA-crystals proceeds in two distinct regimes:

(a) For conversions below 60 % the polymerization occurs in a homogeneous single phase.

(b) Above 60% conversion polymerization proceeds slowly in a new phase, the transition from the initial to the final structure leading to the disruption of the macroscopic crystals.

The nucleation of the new phase in TCDA crystals results from the strain built up during the initial homogeneous polymerization but is also dependent on the occurence of defects in the crystals. Thus it was possible, even at very high radiation doses, to find small undeformed crystals of the initial phase. Almost complete conversion of the material to the new structure occurs when irradiated samples are mechanically deformed.

The homogeneous polymerization is similar to that observed in the phenazine complexes of the 2,4-diynoic acids. However, in these materials the initial single-crystal structure is retained above 60 % conversion but the polymerization rate falls to zero, further irradiation primarily producing cross-linking and some degradation. In TCDA, after the strain has been relieved by the phase transition, further polymerization is possible in addition to other radiation induced processes. Though the macroscopic order of the TCDA crystals is destroyed by the phase transition, much of the material retains order on a smaller scale as evidenced by our microscopic and spectroscopic observations.

Although the polymerization behaviour of TCDA is typical for the series of 10, 12-diynoic acids differing in the number of CH_2-groups in the aliphatic chain, it is not identical with that of the salts of these acids. Resonant Raman and transmission spectroscopy studies of the TCDA–Cd-salt in multilayers [17] and the TCDA–Li-salt in bulk [47, 49] show that in these compounds the phase transition is more complicated and involves at least one intermediate state.

Acknowledgements

This work was supported by a grant from the Science Research Council. We thank Dr D. N. Batchelder for help in recording Raman spectra and Dr M. B. Hursthouse for help with the X-ray diffraction measurements. Useful discussions with them, other members of the Polymer Research group at Queen Mary College and Professor G. Wegner of the University of Freiburg, West Germany, are gratefully acknowledged.

References

1. G. WEGNER, *Z. Naturforsch.* **B24** (1969) 284.
2. *Idem, Faraday Disc.* **68** (1980) 494.
3. D. BLOOR, in "Developments in Crystalline Polymers" edited by D. C. Bassett (Applied Science Publishers, London) in press.
4. R. H. BAUGHMAN and R. R. CHANCE, *Ann. New York Acad. Sci.* **313** (1978) 705.
5. G. WEGNER, in "Molecular Metals" edited by W. E. Hatfield (Plenum Press, New York, 1979) p. 209.

6. D. BLOOR, in "Recent Advances in the Quantum Theory of Polymers" edited by J. M. Andre, J. L. Bredas, J. Delhalle, J. Ladik, G. Leroy and C. Moser (Springer-Verlag, Berlin, 1980) p. 14.
7. J. M. THOMAS, *Pure Appl. Chem.* **51** (1979) 1065.
8. G. M. J. SCHMIDT, "Solid State Photochemistry" (Verlag Chemie, Weinheim/Bergstr., 1976) p. 93.
9. G. SCHEIBE and H. SCHULLER, *Z. Elektrochem.* **59** (1955) 861.
10. D. NAEGELE and H. RINGSDORF, *J. Polymer Sci. Polymer Chem. Ed.* **15** (1977) 2821.
11. B. TIEKE, G. WEGNER, D. NAEGELE and H. RINGSDORF, *Angew. Chem. Int. Ed.* **15** (1976) 764.
12. B. TIEKE, H.-J. GRAF, G. WEGNER, B. NAEGELE, H. RINGSDORF, A. BANERJIE, D. DAY and J. B. LANDO, *Colloid Polymer Sci.* **255** (1977) 521.
13. K. LOCHNER, H. BASSLER, B. TIEKE and G. WEGNER, *Phys. Stat. Solidi* **B88** (1978) 653.
14. B. TIEKE and G. WEGNER, *Makromol. Chem.* **179** (1978) 1693.
15. B. TIEKE, G. LIESER and G. WEGNER, *J. Polymer Sci. Polymer. Chem. Ed.* **17** (1979) 1631.
16. J. P. FOUASSIER, B. TIEKE and G. WEGNER, *Israel J. Chem.* **18** (1979) 227.
17. B. TIEKE and D. BLOOR, *Makromol. Chem.* **180** (1979) 2275.
18. B. TIEKE, G. LIESER and G. WEGNER, *Thin Solid Films* **68** (1980) 77.
19. B. TIEKE, V. ENKELMANN, H. KAPP, G. LIESER and G. WEGNER, *J. Macromol Sci.* **A15** (1981) 1045.
20. B. TIEKE and G. LIESER, *J. Coll. Int. Sci.* **83** (1981) 230.
21. D. DAY and H. RINGSDORF, *J. Polymer Sci. Polymer Lett. Ed.* **16** (1978) 205.
22. D. DAY, H. H. HUB and H. RINGSDORF, *Israel J. Chem.* **18** (1979) 325.
23. H. H. HUB, B. HUPFER, H. KOCH and H. RINGSDORF, *Angew. Chem. Int. Ed.* **19** (1980) 938.
24. P. S. VINCENT and G. G. ROBERTS, *Thin Solid Films* **68** (1980) 135.
25. K. K. KAN, M. C. PETTY and G. G. ROBERTS, in "Physics of MOS Insulators" edited by G. Lucovsky, S. T. Pantiledes and F. L. Galeener (Pergamon Press, Oxford, 1980) p. 344.
26. C. W. PITT and L. M. WALPITA, *Thin Solid Films,* **68** (1980) 101.
27. D. DAY and J. B. LANDO, *Macromolecules* **13** (1980) 1478.
28. B. TIEKE and G. WEGNER, *Makromol. Chem.* **179** (1978) 2573.
29. F. BRAUNSCHWEIG and H. BÄSSLER, *Ber. Bungsenges. Phys. Chem.* **84** (1980) 177.
30. B. TIEKE and D. BLOOR, *Makromol. Chem.* **182** (1980) 133.
31. A. BANERJIE and J. B. LANDO, *Polymer Preprints* **19** (1978) 170.
32. A. CASTILLE, *Liebigs Ann.* **543** (1940) 104.
33. G. C. STEVENS and D. BLOOR, *J. Polymer Sci. Polymer. Phys. Ed.* **13** (1975) 2411.
34. D. J. ANDO, D. BLOOR, C. L. HUBBLE and R. L. WILLIAMS, *Makrol. Chem.* **181** (1980) 453.
35. A. I. KITAIGORODSKI, "Organic Chemical Crystalography" (Consultants Bureau, New York, 1961) p. 181.
36. R. H. BAUGHMAN, *J. Polymer. Sci. Polymer. Phys. Ed.* **12** (1974) 1511.
37. G. WEGNER, *Pure Appl. Chem.* **49** (1977) 443.
38. D. BLOOR, L. KOSKI and G. C. STEVENS, *J. Mater. Sci.* **10** (1975) 1689.
39. R. J. YOUNG, D. BLOOR, D. N. BATCHELDER and C. L. HUBBLE, *ibid.* **13** (1978) 62.
40. R. J. YOUNG, R. DULNIAK, D. N. BATCHELDER and D. BLOOR, *J. Polymer. Sci. Polymer. Phys. Ed.* **17** (1979) 1325.
41. D. BLOOR, F. H. PRESTON, D. J. ANDO and D. N. BATCHELDER, in "Structural Studies of Macromolecules by Spectroscopic Methods" edited by K. J. Ivin (J. Wiley and Sons, New York, 1976) p. 91.
42. W. F. LEWIS and D. N. BATCHELDER, *Chem. Phys. Lett.* **60** (1979) 232.
43. C. BUBECK, W. HERSHEL, W. NEUMANN, H. SIXL and J. WALDMANN, *Chem. Phys.* **72** (1980) 10.
44. D. BLOOR and C. L. HUBBLE, *Chem. Phys. Lett.* **56** (1978) 89.
45. G. R. STROBL, *Colloid Polymer Sci* **254** (1976) 170.
46. D. N. BATCHELDER and D. BLOOR, *J. Phys. C* **11** (1978) L629.
47. B. TIEKE, PhD thesis, University of Freiburg (1978).
48. D. BLOOR, D. N. BATCHELDER, D. J. ANDO, R. T. READ and R. J. YOUNG, *J. Polymer Sci. Polymer Phys. Ed.* **19** (1981) 321.
49. D. BLOOR and B. TIEKE, unpublished work (1981).

Received 21 August
and accepted 19 September 1981